[8] G Protein-Coupled Receptor Internalization Assays in the High-Content Screening Format

By DOROTHEA HAASEN, ANDREAS SCHNAPP, MARTIN J. VALLER, and RALF HEILKER

Abstract

High-content screening (HCS), a combination of fluorescence microscopic imaging and automated image analysis, has become a frequently applied tool to study test compound effects in cellular disease-modeling systems. This chapter describes the measurement of G protein-coupled receptor (GPCR) internalization in the HCS format using a high-throughput, confocal cellular imaging device. GPCRs are the most successful group of therapeutic targets on the pharmaceutical market. Accordingly, the search for compounds that interfere with GPCR function in a specific and selective way is a major focus of the pharmaceutical industry today. This chapter describes methods for the ligand-induced internalization of GPCRs labeled previously with either a fluorophore-conjugated ligand or an antibody directed against an N-terminal tag of the GPCR. Both labeling techniques produce robust assay formats. Complementary to other functional GPCR drug discovery assays, internalization assays enable a pharmacological analysis of test compounds. We conclude that GPCR internalization assays represent a valuable medium/high-throughput screening format to determine the cellular activity of GPCR ligands.

Introduction

Fluorescence microscopy has been widely employed in academic cell biology research as a nondestructive and sensitive technique to visualize subcellular structures and to monitor intracellular protein translocations. In recent years, the pharmaceutical industry has displayed an increasing preference to apply cell biological test systems in the early drug discovery process. Particularly, a novel technique generally referred to as high-content screening (HCS) has been introduced that combines high-resolution fluorescence microscopy with automated image analysis (Almholt *et al.*, 2004; Conway *et al.*, 1999; Ghosh *et al.*, 2000; Li *et al.*, 2003; Taylor *et al.*, 2001). The biomolecules of interest are labeled with different fluorophores that may be monitored in parallel at different wavelengths (multiplexing). Image analysis software quantifies the distribution and brightness of the

METHODS IN ENZYMOLOGY, VOL. 414

0076-6879/06 $35.00
DOI: 10.1016/S0076-6879(06)14008-2

fluorophore-labeled biomolecules in the cells. In a kinetic mode, this enables the visualization of intracellular protein trafficking as a consequence of a pharmaceutical drug effect.

Apart from protein trafficking (Almholt *et al*., 2004), HCS can provide information on the phosphorylation state of target proteins (Russello, 2004), on cellular proliferation (Bhawe *et al*., 2004) or apoptosis (Steff *et al*., 2001), on morphological changes such as neurite outgrowth (Simpson *et al*., 2001), on modifications of the cytoskeleton (Giuliano, 2003; Olson and Olmsted, 1999), on cellular movements (Soll *et al*., 2000), and on other overall changes of the fluorescence such as for the analysis of gap junctions (Li *et al*., 2003).

By these means, HCS provides several advantages over normal high-throughput screening (HTS). Cellular HTS conventionally monitors the mean response of the whole cell population of a microtiter plate (MTP) well. In contrast, HCS can distinguish the individual response of many cells in an MTP well that may differ with respect to the differentiation, the stage of the cell cycle, the state of transfection, or due to natural variability. As a result, heterogeneous pharmaceutical drug effects on mixed cell populations may be analyzed in a single MTP well. ''On-target'' drug effects may be cross-correlated with other phenomena such as cellular toxicity (Wolff *et al*., 2006). Compound artefacts such as cell lysis or compound autofluorescence may be detected. HCS permits work with endogenous targets and/or primary cells using specific antibodies or morphological image analysis. In this way, novel assay formats can be enabled that do not depend on an overall change of fluorescence or luminescence intensity from the whole MTP well.

High-Throughput Confocal Cellular Imaging Systems

HCS has benefited from the introduction of high-throughput confocal cellular imaging systems. In confocal optics, the spatial resolution in the vertical direction is improved dramatically by reducing background fluorescence from above or below the focal plane. This way, confocality enables the observation of cells that adhere to the bottom of a microtiter plate well without interference from dead cells, free fluorophore, or autofluorescent particles above the cellular layer. This increased optical resolution is particularly important to permit the visualization of biomolecule translocation processes across the complex subcellular membrane, vesicle, and organelle systems within eukaryotic cells.

In classic confocal optics (Wilson, 1990), the restriction to fluorescence emission from a specific focal plane is achieved by guiding the emitted light through a pinhole. Using this so-called ''point scanning,'' the fluorescence

emission from a femtoliter-sized observation volume within the focal plane is guided to the photon detector. However, the available confocal point scanning microscopes, which are based on this optical assembly, are generally too slow for drug screening applications.

Three fluorescence microscopic cellular imagers combine a high throughput with confocal optics (Zemanova *et al.*, 2003): the INCell Analyzer 3000 (Glaser, 2004; Haasen *et al.*, 2006) from GE Healthcare Biosciences (Little Chalfont, United Kingdom), the Opera (Eggeling *et al.*, 2003) from Evotec Technologies GmbH (Hamburg, Germany), and the Pathway Bioimager (Vanek and Tunon, 2002) from Becton-Dickinson Bioimaging Systems (Rockville, MD). To reduce measuring time, the Opera and the Pathway Bioimager employ a Nipkow disk (Nakano, 2002) to project fluorescence from several confocal volumes in parallel to a charged-coupled device (CCD) camera, whereas the INCell Analyzer 3000 employs line scanning (Glaser, 2004) through a confocal slit. The imaging and image analysis for the examples given in this chapter are described for the INCell Analyzer 3000.

The INCell Analyzer 3000 provides three laser lines for fluorescence excitation: two (364 nm, 488 nm) from an argon ion laser and one (647 nm) from a krypton laser (Fig. 1). The three laser lines are individually guided through neutral density filters but may be combined for parallel excitation. After reflection by a beam splitter they are autofocused via a 40× Nikon ELWD Plan Fluor/0.6 NA objective to the adherent cell layer at the bottom of the assay MTP well. The 40× Nikon extra-long working distance (ELWD) Plan Fluor/0.6 NA objective provides the combined benefits of a large field of view (FOV; 0.56 mm^2) with a good optical resolution. Fluorescence emission light is collected through the same objective, passed through the aforementioned beam splitter, and guided through a confocal slit. The confocal slit serves to exclude emission light from above or below the focal layer. The light is split into up to three wavelength ranges, which permits simultaneous confocal imaging using three 12-bit −35° cooled CCD cameras. Prior to cellular imaging, a flat field correction for inhomogeneous illumination of the scanned area is carried out using an MTP well containing a homogeneous fluorophore solution.

GPCR Internalization Assays

GPCRs are seven-transmembrane helix proteins (Ji *et al.*, 1998), typically transmitting an extracellular signal into the cell by the conformational rearrangement of their helices and by the subsequent binding and activation of an intracellular heterotrimeric G protein (Perez and Karnik, 2005). In this way, GPCRs act as sensors of exogenous signals, which they transduce into

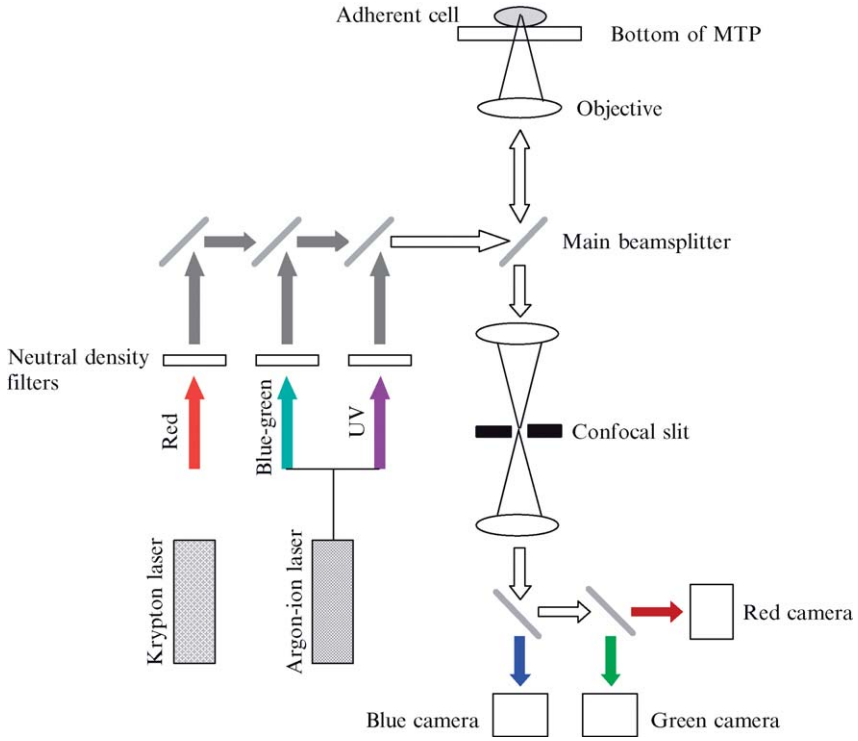

FIG. 1. Optical buildup of the IN Cell Analyzer 3000. The IN Cell Analyzer 3000 employs line scanning through a confocal slit. Two laser lines (364 and 488 nm) from an argon ion laser and one laser line (647 nm) from a krypton laser are guided individually through neutral density filters. All three laser lines may then be combined. After reflection by a beam splitter they are autofocused via a 40× Nikon extra-long working distance (ELWD) Plan Fluor/0.6 NA objective to the adherent cell layer in the assay MTP. Emission light is collected through the same objective, passed through the above beam splitter, and guided through a confocal slit. The light is then split into up to three wavelength ranges, which allows simultaneous confocal imaging using three 12-bit -35° cooled CCD cameras.

cytoplasmic signaling pathways. The first GPCRs to be cloned were bovine opsin (Nathans and Hogness, 1983) and the β-adrenergic receptor (Dixon *et al.*, 1986). Since then, a large gene family of a further ~2000 GPCRs has been reported, classified into more than 100 subfamilies according to sequence homology, ligand structure, and receptor function.

GPCRs are the most important class of therapeutic targets (Ma and Zemmel, 2002). Approximately 45% of all known pharmaceutical drugs

are directed against transmembrane receptors (Drews, 2000), largely against GPCRs. GPCRs are involved in a broad diversity of physiological functions, such as pain perception, chemotaxis, neurotransmission, cardiovascular actions, and metabolism, and finding ways to modulate GPCR signaling remains a major focus of pharmaceutical research.

The interaction between GPCRs and their extracellular ligands has proven to be an attractive point of interference for therapeutic agents. For that reason, the pharmaceutical industry has developed biochemical drug discovery assays to investigate these ligand–GPCR interactions, such as scintillation proximity assays (Alouani, 2000) or the less frequently employed fluorescence polarization assays (Banks and Harvey, 2002; Harris *et al*., 2003) and fluorescence intensity distribution analysis assays (Auer *et al*., 1998; Zemanova *et al*., 2003). All the aforementioned biochemical binding assays rely on the competition of the test compound with a labeled reference ligand. An obvious disadvantage of these binding assays is the risk of missing noncompetitive, allosteric ligands. Further, the binding assay does not elucidate functional aspects of test compound activity, such as full/partial agonism, neutral antagonism, inverse agonism, or positive modulation. To expand compound testing in this direction, there is a need for functional high-throughput assays, possibly measuring GPCR activity in a more physiological, cellular background.

GPCR signal transduction mechanisms have been characterized in three major classes: Gq (phospholipase C), Gi, and Gs (inhibition and stimulation of cAMP production, respectively).

If the GPCR of interest signals via phospholipase C, the most broadly applied cell-based technique to measure GPCR activation is the Ca release assay, either measured in a fluorescent format using Ca-sensitive fluorophores (Sullivan *et al*., 1999) or in a luminescent format using aequorin and a chemiluminescent substrate (Dupriez *et al*., 2002). Alternatively, if the GPCR of interest signals via adenylate cyclase, the cytosolic cyclic adenosine monophosphate (cAMP) content may be determined using various detection technologies (Gabriel *et al*., 2003).

Apart from the aforementioned assays measuring the cellular signaling via G proteins, the functional activation of GPCRs may be monitored by agonist-induced receptor internalization (Milligan, 2003). The broad applicability of GPCR internalization assays (Fig. 2; scheme of GPCR internalization) is based on the common phenomenon of GPCR ''desensitization'' and has been demonstrated for numerous GPCRs (Ferguson, 2001; Krupnick and Benovic, 1998; Oakley *et al*., 2002). In the desensitization process, *GPCR kinases* (GRKs) phosphorylate agonist-activated GPCRs on serine and threonine residues. Arrestins are cytoplasmic proteins that are recruited to the plasma membrane by GRK-phosphorylated GPCRs (Barak *et al*., 1997).

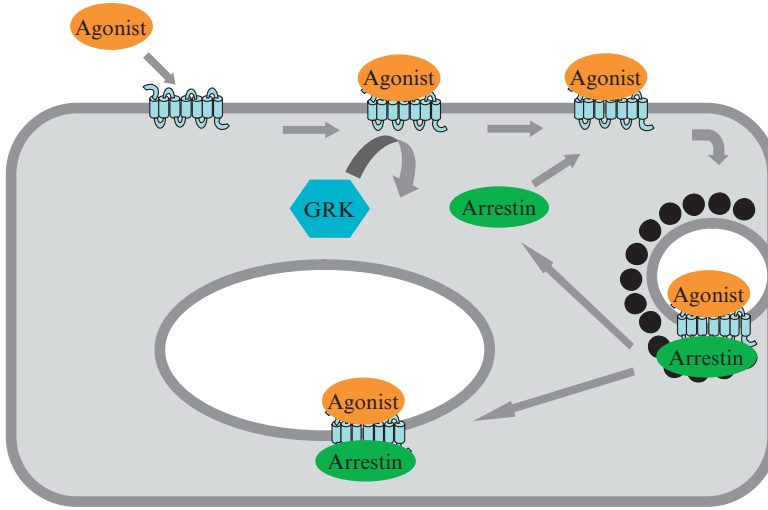

FIG. 2. Scheme of GPCR internalization assays. After agonist stimulation, the GPCR becomes phosphorylated by a GRK on its carboxy-terminal tail. Arrestin is recruited to the plasma membrane by the GRK-phosphorylated GPCR. Arrestin then targets the GPCR to clathrin-coated pits for endocytosis. Depending on the stability of the specific GPCR–arrestin interaction, arrestin is either released after the formation of clathrin-coated pits or cointernalized with the GPCR-loaded vesicles. The internalization process may be monitored by a fluorophore label on the agonist, on the N or C terminus of the GPCR, or on the arrestin.

Arrestins then uncouple the GPCR from the cognate G protein (Lohse *et al.*, 1992; Pippig *et al.*, 1993) and target the desensitized receptors to clathrin-coated pits for endocytosis (Goodman *et al.*, 1996; Laporte *et al.*, 2000).

In contrast to Ca release and cAMP assays, the internalization assay is independent of the individual GPCR intracellular signaling route. Thus, desensitization occurs independently of the associated G protein subclass or of the class of GPCR ligand. Further, the imaging-based GPCR internalization assays offer the general advantages of the HCS format as described earlier.

Internalization Assay and Image Analysis Protocols

Fluorophore-Labeled Ligand Internalization

One means to monitor the internalization of a GPCR is to cointernalize a specific, fluorophore-labeled ligand. In the following example protocol a tetramethylrhodamine-labeled endothelin-1 (TMR-ET-1) is used as a

ligand for the endothelin A receptor (ET_AR). Physiologically, ET_AR is a GPCR that mediates the vasoconstrictive effects of the ET-1 peptide hormone (Bremnes *et al.*, 2000; Yanagisawa *et al.*, 1988).

Materials

Cell lines: hET_A-C1 (high expression level, B_{max} 60–150 pmol/mg protein) and hET_A-C2 (low expression level, B_{max} 17 pmol/mg protein) in CHO-K1 background (Euroscreen)

TMR-ET-1: Custom labeling (Evotec OAI, Hamburg, Germany) with 5-carboxy TMR on the side chain of the lysine in the ET-1 peptide CSCSSLMDKECVYFCHLDII. Dissolve lyophilized product in dimethyl sulfoxide (DMSO) and store in aliquots at −80°.

ET-1, unlabeled: Dissolve lyophilized product (Bachem Feinchemikalien, Bubendorf, Switzerland) in DMSO and store in aliquots at −80°.

Assay plate: black 96-well Viewplate, 800 μm plastic bottom, coated with collagen I (Perkin Elmer)

Complete medium: Ham's F12 supplemented with 10% fetal calf serum

High control: 4 n*M* TMR-ET-1, 0.6% DMSO in assay buffer

Low control: 4 n*M* TMR-ET-1 + 40 n*M* unlabeled ET-1, 0.6% DMSO in assay buffer

Assay buffer: Hank's balanced salt solution (HBSS)/HEPES (1.26 m*M* $CaCl_2$, 0.493 m*M* $MgCl_2$, 0.407 m*M* $MgSO_4$, 5.33 m*M* KCl, 0.441 m*M* KH_2PO_4, 4.17 m*M* $NaHCO_3$, 137.93 m*M* NaCl, 0.338 m*M* Na_2HPO_4, 5.56 m*M* D-glucose,10 m*M* HEPES, pH 7.4), supplemented with 0.2% bovine serum albumin

Fixing solution: 2% formaldehyde, 10 m*M* HEPES in Ham's F12 medium

Phosphate-buffered saline (PBS): 2.67 m*M* KCl, 1.47 m*M* KH_2PO_4, 137.93 m*M* NaCl, 8.06 m*M* Na_2HPO_4

Ligand Cointernalization Protocol

1. Seed cells into assay plate using a multichannel pipette at a density of 25,000 cells in a volume of 100 μl volume per well in complete medium. Culture for 20 to 24 h at 37°, 5% CO_2.
2. Remove complete medium and add 40 μl of ligand in HBSS/HEPES.
3. Incubate assay plate at room temperature.
4. Add 1 volume 2× concentrated fixing solution to wells at indicated time points (t = 10 min, 3.5 h, 8 h).
5. Fix for 30 min at room temperature.
6. Remove fixing solution and add 100 μl PBS.

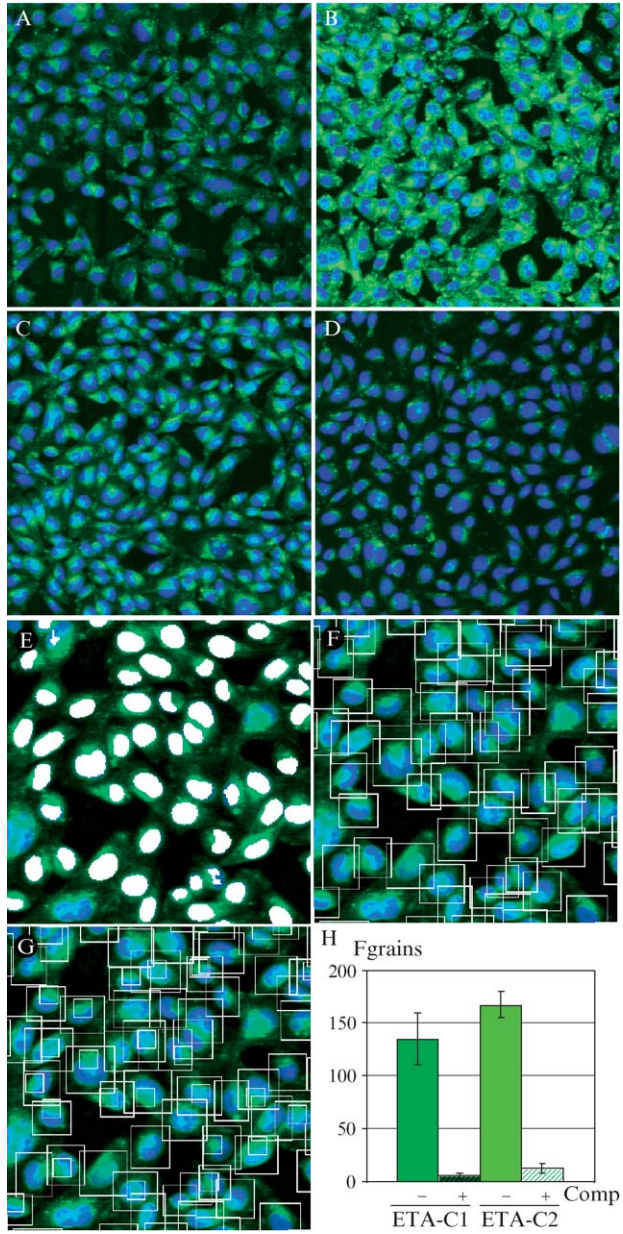

FIG. 3. TMR-ET-1 cointernalization by ETAR. CHO-K1 cells stably expressing medium levels of ETAR (ETA-C2) are stimulated with 4 n*M* TMR-ET-1 (A–C) or 4 n*M* TMR-ET-1 + 40 n*M* ET-1 (D) incubated at room temperature and fixed at 10 min (A), 3.5 h (B), and 8 h (C and D) poststimulation. Fixed cells are imaged on the IN Cell Analyzer 3000 and analyzed

Imaging. For this protocol, the fixed cells are imaged on the IN Cell Analyzer 3000 instrument employing the 488-nm laser line (121 mW; attenuated by a neutral density filter to 10%) combined with the 595BP60 emission filter for TMR-ET-1 and the 364-nm laser line (58 mW; attenuated by a neutral density filter to 50%) combined with the 450BP65 emission filter for Hoechst. Fluorescence emission is recorded sequentially in the green and in the blue channel. Prior to cellular imaging, a flat field correction for inhomogeneous illumination of the scanned area is carried out using an MTP well containing 50 n*M* Oregon Green and 20 μM Alexa Fluor 350 solution (Molecular Probes, Inc., Eugene, OR). All measurements are conducted at room temperature.

Figure 3 shows examples of representative images from wells fixed at different time points. The intracellular fluorescence of TMR-ET-1 increases over time (Fig. 3A–C) due to the formation of small endocytic vesicles that accumulate in larger structures close to the nuclear compartment. The cointernalization of labeled ET-1 can be competed with a 10-fold excess of unlabeled ligand (Fig. 3D).

Image Analysis and Quantification. The cointernalization of a fluorophore-labeled ligand with its specific GPCR upon receptor activation results in the formation of grain-like objects within the cell. Here, the granularity analysis module GRN0 of the IN Cell Analyzer 3000 analysis package is used as a method to identify, analyze, and quantify these grain-like structures. The granularity algorithm employs a two-color image composed of a marker channel and a signal channel. The marker channel image (blue) is employed to identify fluorescently stained cell nuclei, to classify each identified nucleus as an object (Fig. 3E), and to define a region of measurement by the dilation of the nuclear mask for each individual cell. In the signal channel image (green) the region of the dilated nuclear mask (Fig. 3F) is then analyzed for the presence of grains. The algorithm defines grains as distinct regions characterized by two parameters: a specific size and a defined intensity difference as compared to the region of the cell immediately surrounding the grains (Fig. 3G). The Fgrain value, which is the scaled measure of the fraction of cellular fluorescence

using the granularity algorithm GRN0 (E–H). Adapted analysis parameter settings are indicated by the nuclear mask (E), the measurement region of the dilated nuclear mask (large boxes; F and G), and the grain regions (small boxes; G). Images represent one-fourth (A–D) and one-sixteenth (E and F) of a full-size image (750 μm $\times$ 750 μm). Quantification of the grain structures (size: 20 pixels, intensity gradient: 2.0) is performed on the basis of Fgrain values for two stable cell lines expressing ETAR, ETA-C1 (high expression level, 60–150 pmol/mg protein), and ETA-C2 (medium expression level, 17 pmol/mg protein) stimulated with 4 n*M* TMR-ET-1 only (comp $-$) or 4 n*M* TMR-ET-1 + 40 n*M* ET-1 (comp $+$). Values are plotted as means of six images $\pm$ SD.

present in the qualifying grains, is used as the numeric output parameter. It is calculated as

$$\text{Fgrain} = \frac{\text{Sum of pixel values in test boxes corresponding to valid grains}}{\text{Sum of pixel values in dilated mask region}} \times 1000$$

The quantification of Fgrains by the granularity algorithm verifies that in two cell lines stably expressing different levels of ET_AR the co-internalization of TMR-ET-1 can be competed by unlabeled ET-1 (Fig. 3H). A 10-fold excess of unlabeled ligand reduced the Fgrain value from approximately 136 to 5 for the highly expressing cell line ETA-C1 and from approximately 167 to 12 for ETA-C2 with slightly reduced expression levels of ET_AR.

Fluorophore-Labeled Antibody (β2AR)

An alternative assay technology to follow the internalization of a GPCR is to cointernalize a specific antibody, directed either against an extracellular domain of the receptor or against an amino-terminal epitope tag. In the following example protocol the internalization of a vesicular stomatitis virus G (VSVG) epitope-tagged human β2AR expressed in HEK-293 cells is described. In this setup, the primary anti-VSVG-antibody is cointernalized with the receptor upon agonist stimulation and, in a second step, is detected by a fluorophore-labeled secondary antibody by immunofluorescence staining of fixed, permeabilized cells. In this way it is possible to determine the extent of agonist behavior. By way of illustration, the response of the β2AR to the partial agonist salmeterol (Sears and Lotvall, 2005) and the full agonist formoterol (Sears and Lotvall, 2005) is shown.

The molecular mechanisms of receptor tolerance summarized earlier have also been shown to be involved in the desensitization of β2AR (Ferguson, 2001; Lefkowitz, 1998; Su *et al.*, 1980). In the context of β2AR the extent of functional desensitization induced by different β-adrenoceptor agonists is variable, and a correlation between agonist efficacy and receptor desensitization has been shown (Benovic *et al.*, 1988; Clark *et al.*, 1999; January *et al.*, 1997, 1998).

Materials

Cell line: VSVG epitope-tagged β2AR (VSVG-β2AR) in HEK293 background (GE Healthcare, Cardiff, UK)

Assay plate: black 384-well 720-μm glass-bottom plate (MatriCal) coated with 5 $\mu g/cm^2$ poly-D-lysine (PDL)

Compound plate/predilution plate: 384-well MTP (REMP)
Complete medium: minimum essential medium (MEM) with Earle's salts and GlutaMAX I supplemented with 10% fetal calf serum (FCS) and 1% nonessential amino acids
High control: 10 μM isoproterenol (Sigma), 0.316% DMSO in complete medium
Low control: 0.316% DMSO in complete medium
Primary antibody: mouse monoclonal anti-VSVG antibody, clone P4D5 (Sigma)
Krebs–Ringer buffer (KRB): 125 mM NaCl, 4.8 mM KCl, 1.2 mM KH_2PO_4, 1.2 mM $MgSO_4$, 1.3 mM $CaCl_2$, 25 mM HEPES, pH 7.4
Fixing solution: 2% formaldehyde, 10 mM HEPES in KRB
PBS: 2.67 mM KCl, 1.47 mM KH_2PO_4, 137.93 mM NaCl, 8.06 mM Na_2HPO_4
Permeabilization solution: 0.1% saponin in PBS
Secondary antibody: anti-mouse AlexaFluor647 (Molecular Probes)

Antibody Cointernalization Protocol

1. Seed cells into an assay plate using a dispenser at a density of 10,000 cells in a volume of 20 μl per well in complete medium. Culture for 20 to 24 h at 37°, 5% CO_2.
2. Prepare an intraplate dilution series (1:3.16) of compounds in DMSO in a compound plate using an eight-tip pipettor.
3. Dilute compound DMSO solutions in complete medium (1:63.2) into a predilution plate using a 384-well pipetting head.
4. Add 20 μl primary antibody in complete medium to assay plate using a dispenser.
5. Bind antibody for 30 min at 37°, 5% CO_2.
6. Transfer 10 μl of prediluted compounds to assay plate using a 384-well pipetting head.
7. Incubate for indicated time point(s) at 37°, 5% CO_2.
8. Add 1 volume 2× concentrated fixing solution to assay plate.
9. Fix for 30 min at room temperature.
10. Wash assay plate three times with PBS.

Imaging. The fixed cells are imaged on the IN Cell Analyzer 3000 instrument employing the 647-nm laser line (114 mW) combined with the 695BP55 emission filter for Alexa Fluor 647 and the 364-nm laser line (60 mW; attenuated by a neutral density filter to 10%) combined with the 450BP65 emission filter for Hoechst. Fluorescence emission is recorded sequentially in the red and in the blue channel. Prior to cellular imaging, a flat field correction for inhomogeneous illumination of the scanned area is

carried out using an MTP well containing 50 n*M* Cy5 solution (GE Healthcare Biosciences) and 50 μM Alexa Fluor 350 solution (Molecular Probes, Inc.). All measurements are conducted at room temperature.

Figure 4 shows representative images of antibody cointernalization in β2AR-expressing cells treated with a full agonist, formoterol, and a partial agonist, salmeterol. Results show that after stimulation with the full agonist, the red fluorescence representing the subcellular localization of β2AR moves from the plasma membrane to at first smaller vesicles (5 to 10 min) and then to larger vesicles (10 to 20 min) that accumulate in a compartment close to the nucleus at 20 to 30 min post stimulation. In contrast, the response to the partial agonist is delayed, starting with the formation of small vesicles at 10 min post stimulation and reaching a maximal response at 30 min post stimulation. Moreover, the partial response can be seen to apply to each individual cell, resulting in two receptor subpopulations: one that internalizes and another that remains localized at the plasma membrane. In the case of activation by either a full or a partial agonist, the total intracellular red fluorescence decreases at 60 min post stimulation and is reduced to almost background levels at 120 min post stimulation, most likely due to targeting to the lysosomal pathway and degradation.

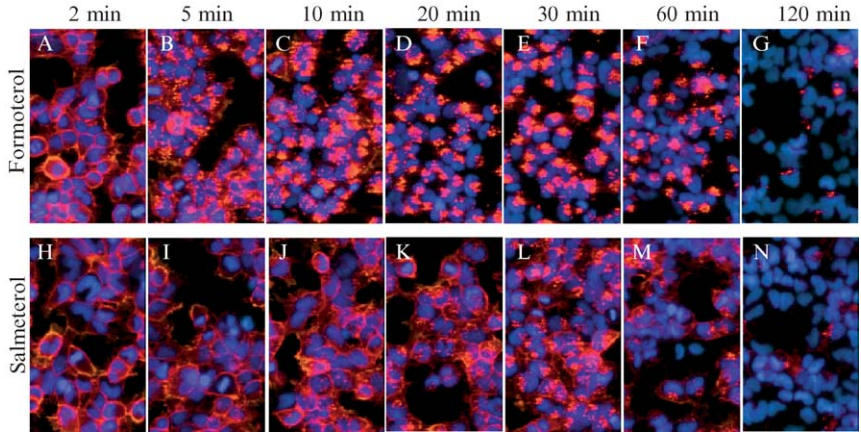

FIG. 4. Antibody cointernalization by β2AR. CHO-K1 cells stably expressing VSVG-tagged β2AR are allowed to bind the anti-VSVG antibody and are stimulated with formoterol (A–G) or salmeterol (H–N) and fixed at 2 min (A, H), 5 min (B, I), 10 min (C, J), 20 min (D, K), 30 min (E, L), 60 min (F, M), and 120 min (G, N) poststimulation. Fixed cells are subjected to immunofluorescence staining by a AF647-labeled secondary antibody and are imaged using the IN Cell Analyzer 3000. Images represent 1/27 of a full-size image (750 $\times$ 750 μm).

Image Analysis and Quantification. Corresponding to the example described in the preceding section for ligand cointernalization experiments, the granularity analysis module GRN0 of the IN Cell Analyzer 3000 analysis package is used as a method to identify, analyze, and quantify the internalized receptor in these experiments. In this case, the red channel image is defined as the signal channel. The GRN0 analysis parameters are optimized for nuclear morphology and the internalization response of the cell line is employed.

Changes in the granular appearance during the endocytic process provide a means to quantify the extent of the cellular response and to distinguish specific stages of endocytosis. Therefore, image analysis is performed setting different sizes and intensity gradients of grain-like objects. Grains are categorized in four subclasses according to their appearance (small, medium, large, and large bright), and their abundance is analyzed over the time course of the experiment (Fig. 5). As a representative example, upon activation by the full agonist formoterol, maximum values of 260 Fgrains are observed, as compared to an Fgrain value of 125 following activation by the partial agonist salmeterol. In case of the full agonist, all grain subclasses are present already 5 min post stimulation, reaching a maximum around 10 min for small, 20 min for medium, and 30 min for large and large bright vesicles (Fig. 5A). In contrast, in the case of the partial agonist, none of the vesicle subclasses are present at 5 min post stimulation, and all subclasses reach their maximum at 30 min post stimulation (Fig. 5B), indicating that the internalization response proceeds differently in comparison to full agonist stimulation.

In Fig. 6, the parameters for medium class vesicles are used to analyze the images from a dose–response experiment for the two agonists. Stimulation with the full agonist results in an efficacy comparable to the standard control isoproterenol (Fig. 6A), whereas the partial agonist reaches only 45% of the maximum response of the standard (Fig. 6B). In this way it can be shown that the antibody cointernalization approach is a sensitive assay system not only to determine EC_{50} values, but also to classify agonists according to their full or partial response.

Conclusions and Outlook

Both the labeled reference ligand internalization and the labeled GPCR internalization methods can produce stable HCS assays. Both formats provide advantageous, partially complementary features in the characterization of GPCR ligand test compounds. Thus, test compounds can be qualified as agonists or antagonists in the ''labeled GPCR'' internalization experiments. In the aforementioned assay protocol for the β2AR, the test

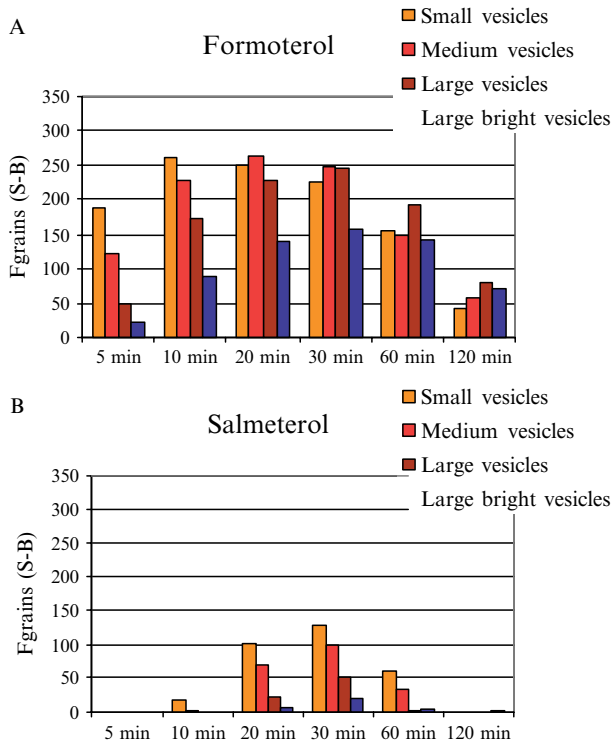

FIG. 5. Quantification of the internalization response of β2AR. Analysis of the grain structures is performed using the granularity analysis module GRN0. Grain objects are classified as follow: small (size: 5 pixels, intensity gradient: 1.5), medium (size: 7 pixels, intensity gradient: 2.0), large (size: 15 pixels, intensity gradient: 2.0), large bright (size: 15 pixels, intensity gradient: 2.5) vesicles. Fgrain values as a mean of two wells per experiment are plotted as S-B (signal from stimulated cells – background from control-treated cells).

compounds are analyzed for their agonistic properties. Alternatively, if the test compounds are preincubated with GPCR expressing cells, the absence of reference agonist-induced GPCR internalization can indicate antagonistic/inverse agonistic properties of the test compound. If the constitutive internalization and recycling rates of the GPCR are sufficient, the inverse agonists may be distinguished from the neutral antagonists by an enrichment of the receptor at the plasma membrane. As a further experimental modification to enable the identification of positive modulators, if the reference agonist is added at approximately EC_{10} concentration, a preincubation

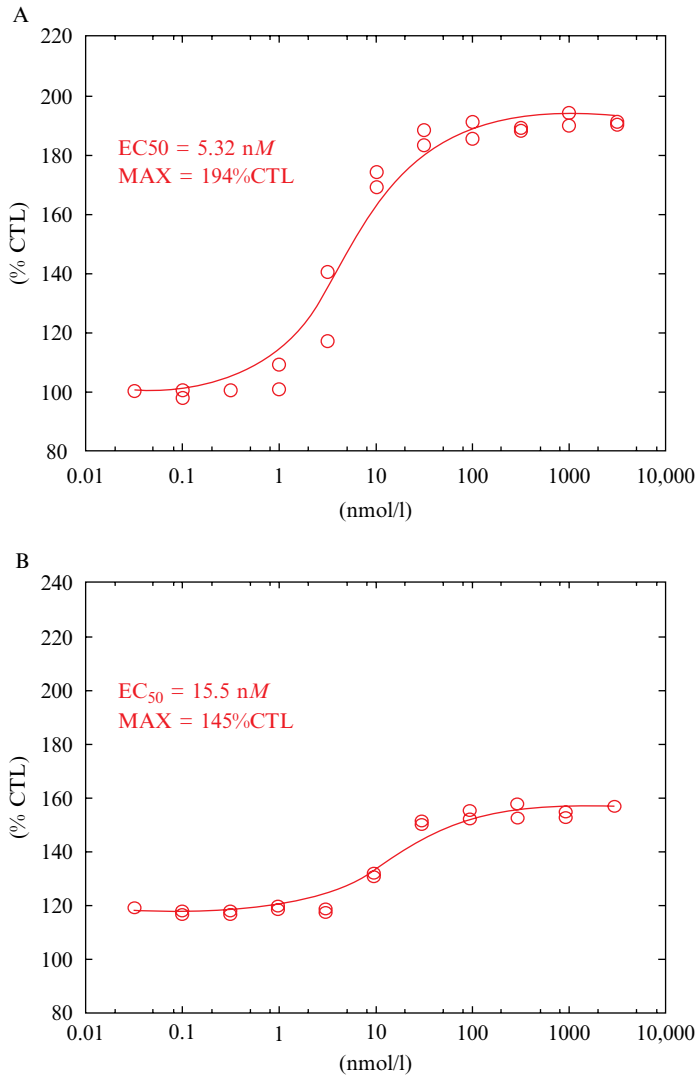

FIG. 6. Full and partial agonist dose response. β2AR-expressing cells are analyzed for medium size vesicles at 10 min poststimulation for formoterol as full agonist (A) and at 20 min poststimulation for salmeterol as partial agonist (B). Dose–response curves and EC_{50}/MAX values are calculated using a customized HTS software product. The assay window is defined by the response to isoproterenol and mock treatment, defining 200 and 100% CTL, respectively.

with a positive modulator compound will increase the internalization rate significantly.

A challenge in GPCR-labeling assays is that antibodies against the extracellular portion of the native receptor are not always available. Further, it is important that the GPCR-labeling antibody does not interfere with the ligand-binding site or produce a functional effect itself. To reduce the probability of such issues, an N-terminal tag may be attached to the GPCR of interest so that a tag-directed antibody may be used for GPCR detection.

In addition to the aforementioned GPCR-labeling assays, the ''labeled ligand'' protocol makes it possible to distinguish between orthosteric and allosteric GPCR-binding test compounds. Orthosterically acting test compounds block the binding of the labeled reference ligand to the cell surface and cannot therefore be analyzed further in ''labeled ligand'' assays. An allosterically acting test compound permits the binding of the labeled reference ligand to the plasma membrane-exposed GPCRs. If the mechanism of action is antagonistic, a preincubation of the allosteric test compound prevents cointernalization of the labeled reference ligand. If the mechanism is positive modulatory, a preincubation of the allosteric test compound leads to an increased rate of labeled ligand internalization. With regard to agonistic, allosteric test compounds, the interpretation of experimental results becomes more challenging: if added at the same time as the labeled reference ligand, depending on the ratio of kinetics, potencies, and efficacies between test compound and reference ligand, the test compounds may either increase or decrease the ''labeled ligand'' internalization rate.

The internalization assays described in this chapter employ an extracellular, ligand/GPCR-labeling step at the plasma membrane. Therefore, the initially increasing number and intensity of intracellular, fluorescent granules describe the rate of receptor internalization. After a few minutes, however, (i) the newly synthesized protein from the secretory pathway reaching the cell surface and (ii) recycling and/or (iii) degradation of ligand- or antibody-labeled GPCRs will be superimposed on the internalization kinetics. To help unravel these complex intracellular receptor trafficking pathways, it is possible to work with a second label that describes the overall distribution of the GPCR, such as a fluorescent protein label at the C terminus of the receptor (Xia *et al.*, 2004) or to use a GPCR-detecting antibody on fixed and permeabilized cells. Such a second label enables observation of the ligand-induced net shift of local GPCR concentrations between the plasma membrane and intracellular compartments. Further, such labeling provides an impression of the GPCR distribution in the cells prior to ligand stimulation, thereby facilitating the overall investigation of test compound-induced changes.

The option to use fixed-cell internalization endpoint protocols, as described earlier for the model system of the β2A receptor, is advantageous

for automated liquid handling and offline imaging. Thus, receptor internalization assays can provide robust medium and/or high-throughput screening formats and excellently complement the drug discovery tool spectrum for the GPCR target class.

Acknowledgment

We thank Paolo Meoni from Euroscreen S.A. (Brussels, Belgium) for providing the ETAR-overexpressing CHO cells that were used in this chapter.

References

Almholt, D. L., Loechel, F., Nielsen, S. J., Krog-Jensen, C., Terry, R., Bjorn, S. P., Pedersen, H. C., Praestegaard, M., Moller, S., Heide, M., Pagliaro, L., Mason, A. J., Butcher, S., and Dahl, S. W. (2004). Nuclear export inhibitors and kinase inhibitors identified using a MAPK-activated protein kinase 2 redistribution screen. *Assay Drug Dev. Technol.* **2,** 7–20.

Alouani, S. (2000). Scintillation proximity binding assay. *Methods Mol. Biol.* **138,** 135–141.

Auer, M., Moore, K. J., Meyer-Almes, F. J., Guenther, R., Pope, A. J., and Stoeckli, K. (1998). Fluorescence correlation spectroscopy: Lead discovery by miniaturized HTS. *Drug Discov. Today* **3,** 457–465.

Banks, P., and Harvey, M. (2002). Considerations for using fluorescence polarization in the screening of G protein-coupled receptors. *J. Biomol. Screen.* **7,** 111–117.

Barak, L. S., Ferguson, S. S., Zhang, J., and Caron, M. G. (1997). A beta-arrestin/green fluorescent protein biosensor for detecting G protein-coupled receptor activation. *J. Biol. Chem.* **272,** 27497–27500.

Benovic, J. L., Staniszewski, C., Mayor, F., Jr., Caron, M. G., and Lefkowitz, R. J. (1988). beta-Adrenergic receptor kinase: Activity of partial agonists for stimulation of adenylate cyclase correlates with ability to promote receptor phosphorylation. *J. Biol. Chem.* **263,** 3893–3897.

Bhawe, K. M., Blake, R. A., Clary, D. O., and Flanagan, P. M. (2004). An automated image capture and quantitation approach to identify proteins affecting tumor cell proliferation. *J. Biomol. Screen* **9,** 216–222.

Bremnes, T., Paasche, J. D., Mehlum, A., Sandberg, C., Bremnes, B., and Attramadal, H. (2000). Regulation and intracellular trafficking pathways of the endothelin receptors. *J. Biol. Chem.* **275,** 17596–17604.

Clark, R. B., Knoll, B. J., and Barber, R. (1999). Partial agonists and G protein-coupled receptor desensitization. *Trends Pharmacol. Sci.* **20,** 279–286.

Conway, B. R., Minor, L. K., Xu, J. Z., Gunnet, J. W., DeBiasio, R., D'Andrea, M. R., Rubin, R., DeBiasio, R., Giuliano, K., DeBiasio, L., and Demarest, K. T. (1999). Quantification of G-protein coupled receptor internatilization using G-protein coupled receptor-green fluorescent protein conjugates with the ArrayScantrade mark high-content screening system. *J. Biomol. Screen* **4,** 75–86.

Dixon, R. A., Kobilka, B. K., Strader, D. J., Benovic, J. L., Dohlman, H. G., Frielle, T., Bolanowski, M. A., Bennett, C. D., Rands, E., and Diehl, R. E. (1986). Cloning of the gene and cDNA for mammalian beta-adrenergic receptor and homology with rhodopsin. *Nature* **321,** 75–79.

Drews, J. (2000). Drug discovery: A historical perspective. *Science* **287,** 1960–1964.

Dupriez, V. J., Maes, K., Le Poul, E., Burgeon, E., and Detheux, M. (2002). Aequorin-based functional assays for G-protein-coupled receptors, ion channels, and tyrosine kinase receptors. *Receptors Channels* **8,** 319–330.

Eggeling, C., Brand, L., Ullmann, D., and Jager, S. (2003). Highly sensitive fluorescence detection technology currently available for HTS. *Drug Discov. Today* **8,** 632–641.

Ferguson, S. S. (2001). Evolving concepts in G protein-coupled receptor endocytosis: The role in receptor desensitization and signaling. *Pharmacol. Rev.* **53,** 1–24.

Gabriel, D., Vernier, M., Pfeifer, M. J., Dasen, B., Tenaillon, L., and Bouhelal, R. (2003). High throughput screening technologies for direct cyclic AMP measurement. *Assay Drug Dev. Technol.* **1,** 291–303.

Ghosh, R. N., Chen, Y. T., DeBiasio, R., DeBiasio, R. L., Conway, B. R., Minor, L. K., and Demarest, K. T. (2000). Cell-based, high-content screen for receptor internalization, recycling and intracellular trafficking. *Biotechniques* **29,** 170–175.

Giuliano, K. A. (2003). High-content profiling of drug-drug interactions: Cellular targets involved in the modulation of microtubule drug action by the antifungal ketoconazole. *J. Biomol. Screen* **8,** 125–135.

Glaser, V. (2004). An interview with Tim Harris, Ph.D. *Assay Drug Dev. Technol.* **1,** 403–408.

Goodman, O. B., Jr., Krupnick, J. G., Santini, F., Gurevich, V. V., Penn, R. B., Gagnon, A. W., Keen, J. H., and Benovic, J. L. (1996). Beta-arrestin acts as a clathrin adaptor in endocytosis of the beta2-adrenergic receptor. *Nature* **383,** 447–450.

Haasen, D., Wolff, M., Valler, M. J., and Heilker, R. (2006). Comparison of G-protein coupled receptor desensitization-related beta-arrestin redistribution using confocal and non-confocal imaging. *Comb. Chem. High Throughput Screen.* **9,** 37–47.

Harris, A., Cox, S., Burns, D., and Norey, C. (2003). Miniaturization of fluorescence polarization receptor-binding assays using CyDye-labeled ligands. *J. Biomol. Screen* **8,** 410–420.

January, B., Seibold, A., Allal, C., Whaley, B. S., Knoll, B. J., Moore, R. H., Dickey, B. F., Barber, R., and Clark, R. B. (1998). Salmeterol-induced desensitization, internalization and phosphorylation of the human beta2-adrenoceptor. *Br. J. Pharmacol.* **123,** 701–711.

January, B., Seibold, A., Whaley, B., Hipkin, R. W., Lin, D., Schonbrunn, A., Barber, R., and Clark, R. B. (1997). beta2-adrenergic receptor desensitization, internalization, and phosphorylation in response to full and partial agonists. *J. Biol. Chem.* **272,** 23871–23879.

Ji, T. H., Grossmann, M., and Ji, I. (1998). G protein-coupled receptors. I. Diversity of receptor-ligand interactions. *J. Biol. Chem.* **273,** 17299–17302.

Krupnick, J. G., and Benovic, J. L. (1998). The role of receptor kinases and arrestins in G protein-coupled receptor regulation. *Annu. Rev. Pharmacol. Toxicol.* **38,** 289–319.

Laporte, S. A., Oakley, R. H., Holt, J. A., Barak, L. S., and Caron, M. G. (2000). The interaction of beta-arrestin with the AP-2 adaptor is required for the clustering of beta 2-adrenergic receptor into clathrin-coated pits. *J. Biol. Chem.* **275,** 23120–23126.

Lefkowitz, R. J. (1998). G protein-coupled receptors. III. New roles for receptor kinases and beta-arrestins in receptor signaling and desensitization. *J. Biol. Chem.* **273,** 18677–18680.

Li, Z., Yan, Y., Powers, E. A., Ying, X., Janjua, K., Garyantes, T., and Baron, B. (2003). Identification of gap junction blockers using automated fluorescence microscopy imaging. *J. Biomol. Screen.* **8,** 489–499.

Lohse, M. J., Andexinger, S., Pitcher, J., Trukawinski, S., Codina, J., Faure, J. P., Caron, M. G., and Lefkowitz, R. J. (1992). Receptor-specific desensitization with purified proteins: Kinase dependence and receptor specificity of beta-arrestin and arrestin in the beta 2-adrenergic receptor and rhodopsin systems. *J. Biol. Chem.* **267,** 8558–8564.

Ma, P., and Zemmel, R. (2002). Value of novelty? *Nature Rev. Drug Discov.* **1,** 571–572.

Milligan, G. (2003). High-content assays for ligand regulation of G-protein-coupled receptors. *Drug Discov. Today* **8,** 579–585.

Nakano, A. (2002). Spinning-disk confocal microscopy: A cutting-edge tool for imaging of membrane traffic. *Cell Struct. Funct.* **27,** 349–355.

Nathans, J., and Hogness, D. S. (1983). Isolation, sequence analysis, and intron–exon arrangement of the gene encoding bovine rhodopsin. *Cell* **34,** 807–814.

Oakley, R. H., Hudson, C. C., Cruickshank, R. D., Meyers, D. M., Payne, R. E., Rhem, S. M., and Loomis, C. R. (2002). The cellular distribution of fluorescently labeled arrestins provides a robust, sensitive, and universal assay for screening of G protein-coupled receptors. *Assay Drug Dev. Technol.* **1,** 21–30.

Olson, K. R., and Olmsted, J. B. (1999). Analysis of microtubule organization and dynamics in living cells using green fluorescent protein-microtubule-associated protein 4 chimeras. *Methods Enzymol.* **302,** 103–120.

Perez, D. M., and Karnik, S. S. (2005). Multiple signaling states of G-protein-coupled receptors. *Pharmacol. Rev.* **57,** 147–161.

Pippig, S., Andexinger, S., Daniel, K., Puzicha, M., Caron, M. G., Lefkowitz, R. J., and Lohse, M. J. (1993). Overexpression of beta-arrestin and beta-adrenergic receptor kinase augment desensitization of beta 2-adrenergic receptors. *J. Biol. Chem.* **268,** 3201–3208.

Russello, S. V. (2004). Assessing cellular protein phosphorylation: High throughput drug discovery technologies. *Assay Drug Dev. Technol.* **2,** 225–235.

Sears, M. R., and Lotvall, J. (2005). Past, present and future: Beta2-adrenoceptor agonists in asthma management. *Respir. Med.* **99,** 152–170.

Simpson, P. B., Bacha, J. I., Palfreyman, E. L., Woollacott, A. J., McKernan, R. M., and Kerby, J. (2001). Retinoic acid evoked-differentiation of neuroblastoma cells predominates over growth factor stimulation: An automated image capture and quantitation approach to neuritogenesis. *Anal. Biochem.* **298,** 163–169.

Soll, D. R., Voss, E., Johnson, O., and Wessels, D. (2000). Three-dimensional reconstruction and motion analysis of living, crawling cells. *Scanning* **22,** 249–257.

Steff, A. M., Fortin, M., Arguin, C., and Hugo, P. (2001). Detection of a decrease in green fluorescent protein fluorescence for the monitoring of cell death: An assay amenable to high-throughput screening technologies. *Cytometry* **45,** 237–243.

Su, Y. F., Harden, T. K., and Perkins, J. P. (1980). Catecholamine-specific desensitization of adenylate cyclase: Evidence for a multistep process. *J. Biol. Chem.* **255,** 7410–7419.

Sullivan, E., Tucker, E. M., and Dale, I. L. (1999). Measurement of [Ca2+] using the fluorometric imaging plate reader (FLIPR). *Methods Mol. Biol.* **114,** 125–133.

Taylor, D. L., Woo, E. S., and Giuliano, K. A. (2001). Real-time molecular and cellular analysis: The new frontier of drug discovery. *Curr. Opin. Biotechnol.* **12,** 75–81.

Vanek, P. G., and Tunon, P. (2002). High-throughput single-cell tracking in real time. *Gen. Eng. News* **22,** 1–4.

Wilson, T. (1990). ''Confocal Microscopy.'' Academic Press, New York.

Wolff, M., Haasen, D., Merk, S., Kroner, M., Maier, U., Bordel, S., Wiedenmann, J., Nienhaus, G. U., Valler, M. J., and Heilker, R. (2005). Automated high content screening for phosphoinositide 3 kinase inhibition using an AKT1 redistribution assay. *Comb. Chem. High Throughput Screen.* **9,** 339–350.

Xia, S., Kjaer, S., Zheng, K., Hu, P. S., Bai, L., Jia, J. Y., Rigler, R., Pramanik, A., Xu, T., Hokfelt, T., and Xu, Z. Q. (2004). Visualization of a functionally enhanced GFP-tagged galanin R2 receptor in PC12 cells: Constitutive and ligand-induced internalization. *Proc. Natl. Acad. Sci. USA* **101,** 15207–15212.

Yanagisawa, M., Kurihara, H., Kimura, S., Tomobe, Y., Kobayashi, M., Mitsui, Y., Yazaki, Y., Goto, K., and Masaki, T. (1988). A novel potent vasoconstrictor peptide produced by vascular endothelial cells. *Nature* **332,** 411–415.

Zemanova, L., Schenk, A., Valler, M. J., Nienhaus, G. U., and Heilker, R. (2003). Confocal optics microscopy for biochemical and cellular high-throughput screening. *Drug Discov. Today* **8,** 1085–1093.